ACS ES&T Water

pubs.acs.org/estwater

Article

# Photocatalytic Degradation of 1,4-Dioxane and Malachite Green over Zinc Oxide/Cellulose Nanofiber Using UVA/B from Direct Sunlight and a Continuous Flow Reactor

Mostafa Dehghani, Mahdi Naseri, Humayun Nadeem, Mark M. Banaszak Holl, and Warren Batchelor*

Cite This: *ACS EST Water* 2022, 2, 786−797

Read Online

ACCESS | Metrics & More | Article Recommendations | Supporting Information

**ABSTRACT:** Concerns over water contamination by biorecalcitrant, persistent organic pollutants have emphasized the need for effective, cheap, and scalable treatment methods. Photocatalysis offers the potential advantages of using air as the oxidant, ambient conditions for reaction, and sunlight as the source of energy; however, identifying a sustainable catalyst support and sunlight-active, earth-abundant photocatalysts is challenging. This study demonstrates for the first time the development of a ZnO/cellulose nanofiber (CNF) continuous flow photoreactor for fast and effective degradation of industrial pollutants 1,4-dioxane and malachite green and model pollutant methylene blue in water. The novel sun-flow reactor consists of open, interconnected parallel channels with a continuous flow of water containing the chosen pollutant circulated over the catalyst under ultraviolet (UV)A/B irradiation from direct sunlight. Mass spectrometry (MS), gas chromatography (GC)-MS, liquid chromatography (LC)-MS, and inductively coupled plasma (ICP)-MS analyses were used to investigate and quantify the extent of degradation and the byproducts formed in the process. Aqueous solutions of 10 ppm methylene blue and malachite green, as well as their reaction byproducts, were reduced below 0.1 ppm (the detection limit) with an energy per order (EE/O) figure of merit of 2.2 kWh/m$^3$ per order. A 3.5 ppm aqueous solution of 1,4-dioxane was reduced to 0.034 ppm with an EE/O figure of merit of 1.6 kWh/m$^3$ per order.

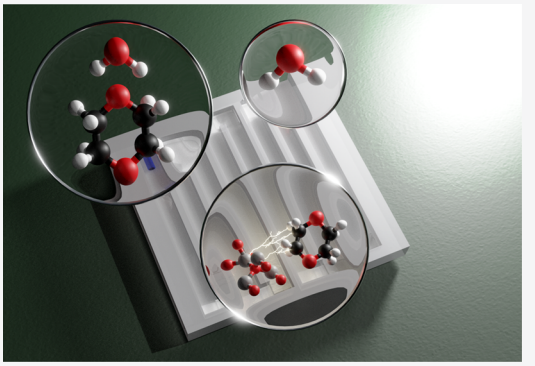

**KEYWORDS:** *1,4-dioxane, malachite green, continuous photoreactor, photocatalytic water remediation, sustainable catalyst, persistent organic pollutant, biorecalcitrant*

Downloaded via MONASH UNIV on November 17, 2025 at 04:57:00 (UTC).
See https://pubs.acs.org/sharingguidelines for options on how to legitimately share published articles.

## INTRODUCTION

The presence of biorecalcitrant, persistent organic pollutants (POPs) in water has become a critical environmental and health issue.[1,2] Standard water treatment methods including filtration, flocculation, chemical oxidation, and biological treatment often fail to fully remove POPs leading to a substantial interest in advance oxidation processes (AOPs) for the removal of these chemicals. Photocatalytic degradation strategies[3−7] have attracted particular attention due to their promise for cost-effective, rapid, and efficient degradation of POPs including the potential for complete mineralization of the contaminants.[8−12] Despite these potential advantages, drawbacks of current technologies preventing broad commercialization include scalability,[13,14] cost of running ultraviolet (UV) and/or visible lamps, use of expensive and non-earth-abundant transition-metal catalysts,[15−17] and testing limited to simple model dyes such as methylene blue (MB).[18]

To address these challenges, earth-abundant catalysts such as ZnO[8,16] and $TiO_2$[14] have been extensively studied. Low photoconversion efficiency continues to remain a major challenge, and this has driven extensive studies focused on catalyst improvement including dopant and coupled semiconductor approaches. Recently, we reported a nanostructured ZnO catalyst capable of natural sunlight-driven photodegradation of methylene blue (MB) dye that addressed the challenge by choice of site (Melbourne, Australia), which provides sufficient radiance in the UVA (3.10−3.94 eV) and UVB (3.94−4.13 eV) range to active the direct band gap (3.37 eV) ZnO without additional modification.[19] In batch mode, this system provided >99% degradation of a 5 ppm solution of MB dye in less than 10 min and exhibited <1% decrease in catalytic function over 10 repeat cycles. Although a promising result, recent reviews in the field such as those by Loeb et al. and Wang et al. have stressed that the photocatalytic literature too often ignores key scale-up challenges,[8,10] and we note that this extends to a lack of consideration of plant site selection

Received: December 16, 2021
Revised: February 28, 2022
Accepted: March 29, 2022
Published: April 8, 2022



© 2022 American Chemical Society



https://doi.org/10.1021/acsestwater.1c00484
*ACS EST Water* 2022, 2, 786−797

Scheme 1. Sun-Flow Photodegradation Apparatus Used for This Study[a]

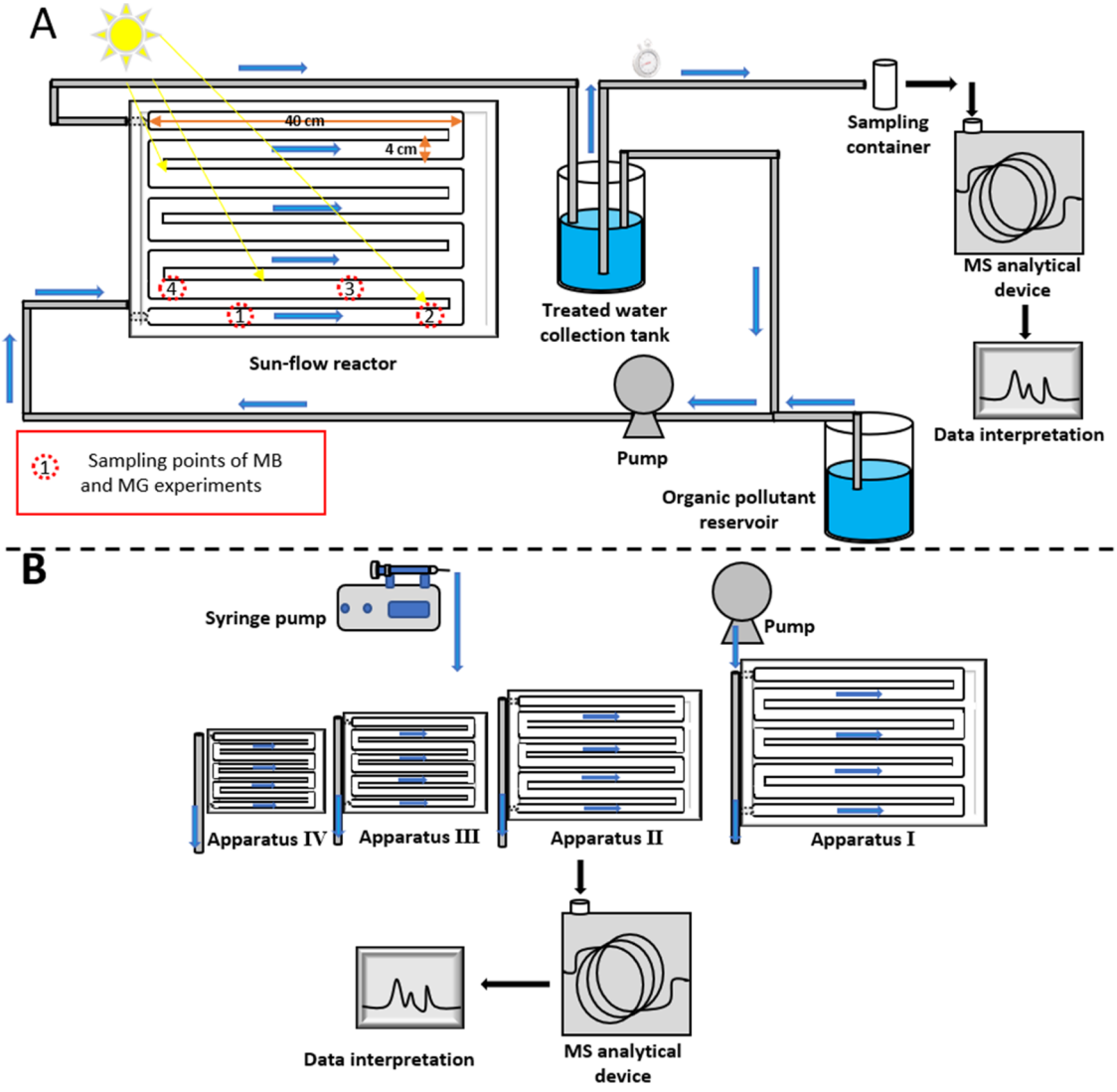


[a](A) Detailed photocatalytic degradation study performed using sun-flow apparatus I identifying 1−4 min sampling points and treated water collection tank use for 1,4-dioxane sampling. (B) Scaling study for apparatus I−IV.

and local solar radiation characteristics. To further probe the effectiveness of ZnO as a water treatment photocatalyst using the natural UVA/B characteristics of the Australian solar radiance, a number of additional key research gaps need to be addressed: expansion to a wider substrate set including nondye molecules,[18] implementation in a scalable flow chemistry configuration, use of a broadly comparable figure of merit such as EE/O, and ability to achieve relevant environmental targets for removal of pollutants. Advancement in these aspects of photocatalytic water treatment is considered to be integral for studies of existing and novel catalysts.

In this study, site-specific solar radiance characteristics are explicitly considered in the context of a simple free-falling film, continuous flow reactor design to ensure capture of both direct and diffuse solar radiation, and excellent oxygen saturation[14] coupled to an easily produced, nanostructured ZnO catalyst.[20,21] ZnO has superior light absorbance properties as compared to $TiO_2$ in the UVA region, making it of particular interest for sites located in Australia or similar UVA/B radiance regions.[22,23] The location is important based on the solar radiation, not the specific location. For ZnO photocatalyst to activate, it is important to have high UVA/B intensity, and as Australia has very high UVA/B, this location can be used as a perfect example. Although using a doping material or coupling ZnO with other semiconductors can improve the visible light activity, usage of only ZnO as the catalyst under direct sunlight has been the biggest challenge in past studies. The cellulose nanofiber (CNF) support, which exhibited excellent performance under batch conditions,[20] was employed as the support for the free-falling film reactor. The vast majority of published ZnO-based photodegradation studies are in batch mode and/or employ dye models as the sole substrate.[8,16] To benchmark both the flow and batch studies in the literature, the commonly studied methylene blue (MB) dye and the more industrially relevant malachite green (MG) dye were employed. MG is a cheap dye employed in the fish farming, textile, and leather industries that is banned in the United States and Europe because of its teratogenic and carcinogenic effects.[24] Although there are not yet specific concentration guidelines and limitations, it is highly recommended to remove it from water.[25] The nondye substrate 1,4-dioxane was selected to test if the observed photocatalytic degradation characteristic of


https://doi.org/10.1021/acsestwater.1c00484
ACS EST Water 2022, 2, 786−797

ZnO under Australian solar radiance was dominated by a dye-sensitized reaction mechanism[18] or was broadly applicable to a wide variety of biorecalcitrant POPs. 1,4-Dioxane is a potential occupational carcinogen that may increase the chance of nasal cavity, gall bladder, and liver tumors[26] and has recently been categorized as an environmental contaminant that is problematic for health.[27] Both 1,4-dioxane and MG are industry-relevant, water-soluble, biorecalcitrant, mobile, and toxic pollutants that easily contaminate ground-water resources.[28,29]

Previously, Lee et al. investigated the photocatalytic degradation of 1,4-dioxane using $TiO_2$ catalysts under UV lamps in a membrane continuous photoreactor achieving a final concentration of 0.04 ppm with the electrical energy per order (EE/O) of 1.9 kWh/m$^3$/order.[30] Mueses et al. studied the photocatalytic degradation of 1,4-dioxane using a compound parabolic collector photoreactor and $TiO_2$ catalyst.[31] They used sunlight as the source of energy and achieved an EE/O of 0.19 kWh/m$^3$/order. Yamazaki et al. investigated the photocatalytic degradation of 1,4-dioxane using continuous annular reactors and $TiO_2$ catalyst under UVC lamp irradiation.[32] They were able to reduce 1,4-dioxane concentration to 0.09 ppm with an EE/O of 2.88 kWh/m$^3$/order. The EE/O figure of merit is therefore employed to compare the performance of the four-reactor scales described in this study to each other as well to previous literature examples.

## EXPERIMENTAL SECTION

**Chemicals.** Methylene blue (MB), malachite green oxalate salt (MG), 1,4-dioxane (reagent plus ≥ 99%), and zinc acetate dihydrate (ACS reagent, purity > 98%) were purchased from Sigma-Aldrich Co., Australia. Cellulose nanofiber (CNF) (KY-100S grade and 25% solid content) was obtained from DAICEL Chemical Industries Limited, Japan. Absolute ethanol was purchased from Ajax Finechem, Australia, and the NaOH dry pellets in analytical/reagent grade were purchased from Merck Co., Germany. Hydrochloric acid 36% was purchased from RCI Labscan Limited, Thailand. Clear acrylic sheets were purchased from acryliconline.com.au online shop. All chemicals were used without further purification.

**Synthesis of ZnO/CNF Catalyst.** The ZnO/CNF catalyst was prepared as described in our previous study.[20] In brief, 120 g of wet CNF (75 wt % moisture content, 30 g of dry CNF, without any further treatment) was added to 1880 g of Milli-Q water (to form 1.5 wt % of dry CNF content suspension) and disintegrated using a Messmer disintegrator (Model MKIIIC, Netherlands) at 3000 rpm for 15,000 revolutions. The resultant suspension was mixed with 126 g of zinc acetate dihydrate powder (to obtain 0.3 M $Zn(OAc)_2$ in a 2 kg of suspension) and mixed using a Dispermat mixer (VMA-Getzmann GMBH) at 2000 rpm for 1 h. Next, 120 g of NaOH pellets were slowly added to the suspension (to produce a 1.5 M NaOH in 2 kg of suspension) and mixed using Dispermat mixer for 3 h at 80 °C to produce a milky white suspension.[33,34] Information regarding pore size and surface area of the catalyst (Brunauer−Emmett−Teller (BET) analysis) can be found in our previous study.[19]

**Construction of the Sun-Flow Apparatus.** The sun-flow apparatus consists of an immobilized ZnO/CNF bed and free-falling film reactor optimized for the direct and diffuse solar radiance in Australia (Scheme 1). Sun-flow apparatus I was constructed out of a clear acrylic sheet (40 × 60 × 2 cm$^3$) that was machined to form parallel channels (40 × 4 × 1.5 cm$^3$) (Scheme 1A, Figures S1 and S2). The ZnO/CNF suspension was cast inside molds made from clear acrylic sheets in the size and shape of the channels and then oven-dried at 105 °C for 3 h to remove all of the moisture from the catalyst. The ZnO-embedded, catalyst support sheets were placed on the bottom of the channels, and the water samples were pumped over them using a MasterFlex L/S pump (Cole-Parmer Instrument Co.) at a flow rate of 16.7 mL/min with a water depth of about 5 mm. Dimensional details of sun-flow apparatus I, and all other apparatus employed in this study, are presented in Table 1. The parallel open-channel, free-falling film design was selected to maximize oxygen saturation, solar flux, the interaction of pollutants with the catalyst, and to provide a gravity water flow.[14] The experiments were conducted under direct sunlight at GPS coordinates of −37.909120 latitude and 145.132686 longitude (Clayton, Victoria, Australia), which provides the UVA solar radiance matched to the ZnO catalyst.

**Table 1. Summary Dimensional Characteristics of the Sun-Flow Apparatus**

| apparatus | channel length (cm) | channel width (cm) | surface area (cm$^2$) | dry ZnO/CNF catalyst/support (g) | flow rate (mL/min) |
|---|---|---|---|---|---|
| I | 40 | 4 | 160 | 11.72 | 16.7 |
| II | 20 | 2 | 40 | 2.93 | 4.2 |
| III | 20 | 0.8 | 16 | 1.17 | 1.7 |
| IV | 8 | 0.8 | 6.4 | 0.47 | 0.7 |

**Photocatalytic Degradation Testing Using Sun-Flow Apparatus I.** The photocatalytic degradation of organic pollutants was tested using MB, MG, and 1,4-dioxane. Sunlight intensity was measured by a ProSciTech Pty Ltd E850009 UVA/B meter (±4% standard deviation). The UVA/B intensity varied during the day, depending on the weather and the sun's position. To normalize the total UVA/B exposure between experiments, sun-flow apparatus type, and as a function of both UVA/B intensity and time, the following equation was used

$$E = t \times I \times A \quad (1)$$

where $E$ is total UVA/B solar energy exposure (kJ), $t$ is the irradiation time (s), $I$ is the average UVA/B intensity over time (kW/m$^2$), and $A$ is the area in contact with UV light on the catalyst/support surface (m$^2$). The experiments were done at pH 11, which was the intrinsic pH of the system without any modification. Water samples (5 mL) were removed from the apparatus at standard intervals for analysis. Sampling is reported as ZnO/CNF contact time (defined as the amount of time flowing solution is in contact with the ZnO/CNF catalyst/support in the bottom of reactor channel) for MB (Figures 1 and 2) and MG (Figure 3) with the solution removed from sun-flow apparatus I at the locations indicated in Scheme 1A. Sampling for 1,4-dioxane is reported as the total ZnO/CNF contact time for the sun-flow apparatus I system with 5 mL of sample solutions removed from the 2 L treated water collection tank at the specified time intervals. To investigate the effect of pH on the photocatalytic degradation of organic pollutants, HCl was used in the MB solutions to adjust the pH between 4 and 14 during the experiments.

**Mass Spectrometry (MS) Analyses.** Except where noted, analyses were carried out at the Monash Analytical Platform, School of Chemistry, Monash University. Qualitative and quantitative LC-MS were used to identify the amount of MB and MG in the samples and the presence of 1,4-dioxane


https://doi.org/10.1021/acsestwater.1c00484
ACS EST Water 2022, 2, 786−797

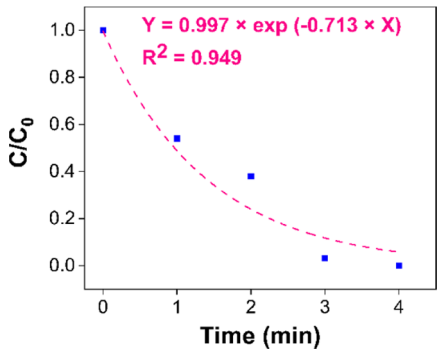


**Figure 1.** Photobleaching of 10 ppm aqueous MB in sun-flow apparatus I as a function of ZnO/CNF contact time. UVA/B intensity average = 40 W/m$^2$, flow rate = 16.7 mL/min, ZnO/CNF catalyst/support used = 11.72 g, and water depth in channels ≈ 5 mm.

byproducts. ICP-MS was used to identify the amount of $Zn^{2+}$(aq) released in water during the course of an experiment. High-resolution (HR)GC-MS was used to identify and quantify the amount of 1,4-dioxane present in samples.

**Qualitative LC/MS/TOF.** LC/MS analysis was conducted on an Agilent 6220 TOF MS system (Santa Clara, CA) with a multimode dual nebulizer electrospray ionization (ESI)/atmospheric pressure chemical ionization (APCI) source. The LC consisted of an Agilent 1200 series solvent degasser, binary pump, column oven, and sample manager. An Agilent SB-C18-bonded silica 1.8 $\mu$M (2.1 × 50 mm$^2$) column was used for the LC/MS study. The mobile phase consisted of MeCN and $H_2O$, both containing 0.1% v/v formic acid, and delivered using a binary gradient over 20 min followed by re-equilibration to the starting conditions. Based on previous literature studies[35−37] and to have enough residence time in the column, the flow rate was set at 0.4 mL min$^{-1}$ and the injection volume was 5 $\mu$L. LC/MS analysis was conducted using both positive and negative ion detection, and elution of the analyte was monitored using the following MS conditions: nebulizer pressure 35 psi, gas flow rate 8 L/min, gas temperature 300 °C, capillary voltage 2500/−2500 V, fragmentor 150, and skimmer 65 V. The instrument was operated in the extended dynamic range mode with data collected in $m/z$ range 50−1000.[35−37]

**Quantitative LC/MS.** Quantitative LC/MS data was generated using an Agilent 1200 series LC (Santa Clara, CA) equipped with a single quad Waters Micromass ZQ MS system (Milford, MA) with an ESI source and an Agilent SB-C18-bonded silica 1.8 $\mu$M (2.1 × 50 mm$^2$) column. The mobile phase consisted of MeCN and $H_2O$, both containing 0.1% v/v formic acid, and delivered using a binary gradient over 20 min followed by re-equilibration to the starting conditions. The flow rate was 0.4 mL min$^{-1}$, and the injection volume was 5 $\mu$L. LC/MS analysis was conducted using positive mode electrospray ionization and elution of the analyte monitored in single ion monitoring (SIM) mode. Concentrations were determined by comparison to a set of calibration standards prepared in a blank solvent.[35−37]

**ICP-MS for Zn Release Test.** $Zn^{2+}$ ion concentration in water was determined using a PerkinElmer NexION 350 inductively coupled plasma mass spectrometer, measuring zinc at 63.93 amu. Raw count rates from the analyses were externally standardized through a calibration curve constructed using a commercially available zinc 64 stock solution supplied by Merck. An internal standard of 80 ppb germanium was used for zinc analysis. $Zn^{2+}$(aq) amount in Milli-Q water was measured as the reference and deducted from the results. Standard zinc solutions with a concentration of 1 ppb to 10 ppm were used to construct the calibration curve.

**High-Resolution Gas Chromatography-Mass Spectrometry (HRGC-MS) for Both Quantitative and Qualitative 1,4-Dioxane Detection.** National Association of Testing Authorities (NATA) accredited analysis of 1,4-dioxane in water was carried out at Eurofins Environment Testing Australia Pty Ltd. using USA-EPA Method 522, which employs isotope dilution HRGC-MS. In brief, as described on the Eurofins Scientific Environmental Testing website (https://www.eurofins.com.au/environmental-testing/water-testing/; accessed 13-9-2021), a splitless injection with a high-resolution fused silica capillary GC column was interfaced to an MS operated in the SIM mode. The analyte, SUR, and IS were separated and identified by comparing the acquired mass spectra and retention times to reference spectra and retention times for calibration standards acquired under identical GC/MS conditions. The concentration of the analyte was determined by comparison to its response to calibration standards relative to the IS.[38]

**Sun-Flow Scaling Study: Apparatus I−IV.** To investigate the scalability of the sun-flow apparatus, four different systems (I−IV: Table 1 and Figure S2) were prepared and tested using 1, 3, 5, 10, and 20 ppm concentrations of model pollutant MB. The flow rates employed for apparatus I−IV of 16.7 (MasterFlex L/S pump (Cole-Parmer Instrument Co.)), 4.2, 1.7, and 0.7 mL/min, respectively, were achieved using a NE-4000 Programmable 2 Channel Syringe Pump, New Era Pump Systems Inc. These flow rates were selected to maintain a laminar flow with a constant Reynolds number of ∼250 in each apparatus. In every case, the MB solutions were allowed to flow until a steady flow state was achieved in the entire apparatus. MB sample contact time for each apparatus was varied using internal physical sampling in a fashion analogous to that described in detail for sun-flow apparatus I in the Photocatalytic Degradation Testing Using Sun-Flow Apparatus I section. Specifically, for sun-flow apparatus I, 0.5 mL of aliquots were sampled at the 1 min ZnO/CNF and the MB solution contact time point (after flow of the MB solution in the system for 1 min and at point 1 in Scheme 1). For sun-flow apparatus II−IV, 0.5 mL of aliquots were sampled at the 0.5 min ZnO/CNF and the MB solution contact time point. The dimensional scale differences required a different contact time point for sun-flow apparatus I, although a common time was possible for apparatus II−IV. The UVA/B intensity average was 45 W/m$^2$ for all experiments. All scaling experiments were carried out at GPS coordinates of −37.909120 latitude and 145.132686 longitude, identical to all other apparatus studies reported herein. A summary of the study and apparatus employed is provided in Scheme 1. The photocatalytic degradation mechanism schematic of organic pollutants in this study using ZnO catalyst based on the mechanism proposed by Lee et al.[8] is illustrated in Scheme 2.

## RESULTS AND DISCUSSION

**Photocatalytic Degradation of Methylene Blue (MB).** The photocatalytic degradation of MB has been widely employed as a model pollutant dye for photodegradation experiments, including recently reported ZnO/CNF studies performed under batch conditions.[8,20] Typically, studies are performed using colorimetric detection to detect photo-


https://doi.org/10.1021/acsestwater.1c00484
ACS EST Water 2022, 2, 786−797

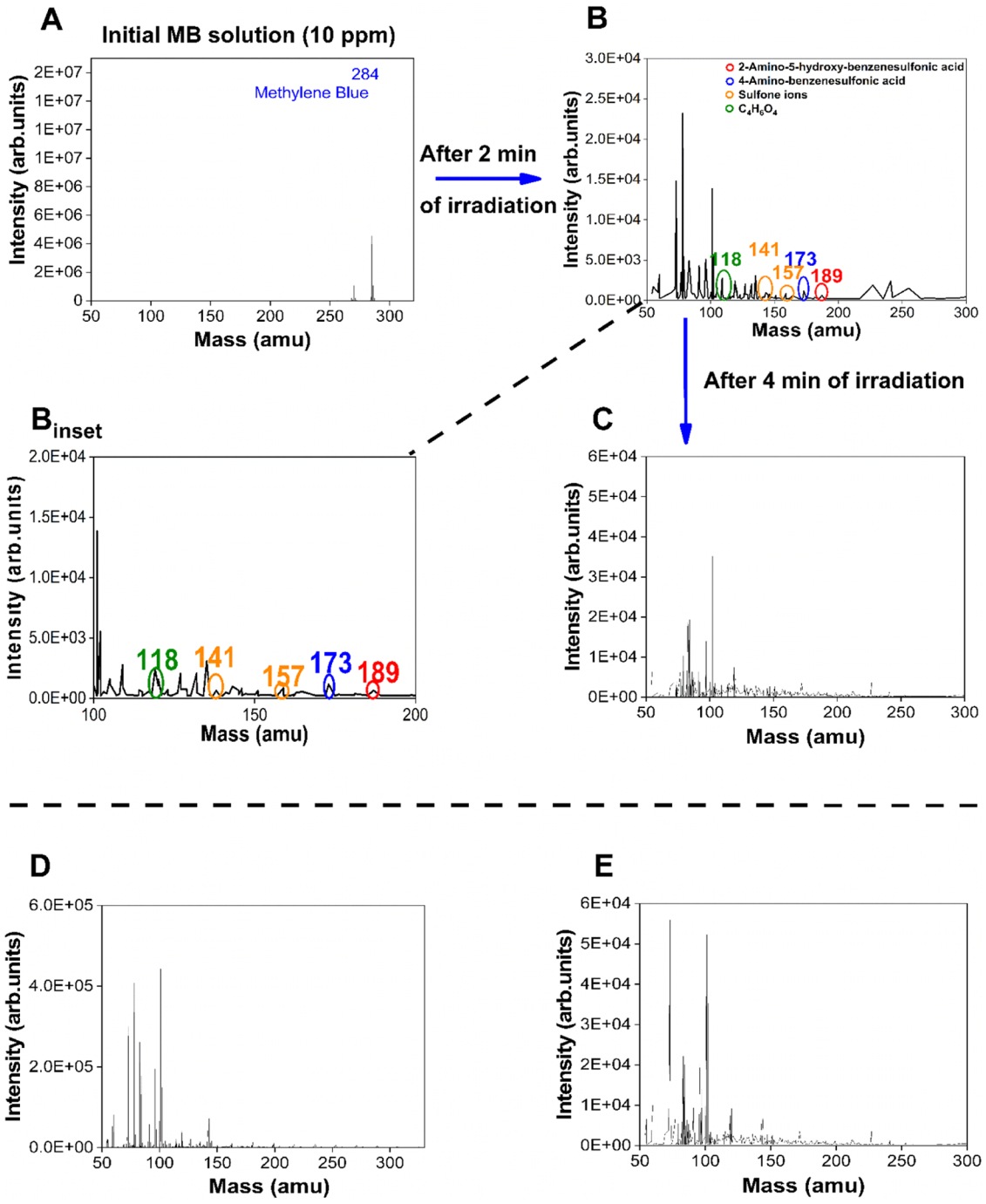


**Figure 2.** LC-MS analysis of 10 ppm aqueous MB samples in sun-flow apparatus I as a function of ZnO/CNF contact time. (A) Untreated, (B) 2 min, (C) 4 min, (D) Milli-Q water reference, and (E) Milli-Q water without MB after 4 min contact time. UVA/B intensity average = 40 W/m$^2$, flow rate = 16.7 mL/min, ZnO/CNF catalyst/support used = 11.72 g, and water depth in channels ≈ 5 mm.

bleaching; however, studies have also been performed examining the chemical identity of MB byproducts.[39,40] For this study, the photocatalytic degradation of MB was investigated using both colorimetric (Figure 1) and LC-MS analysis (Figure 2).[41] In both cases, a 10 ppm aqueous solution of MB was flowed at a rate of 16.7 mL/min over the ZnO/CNF support. The flowing solution exposed to sunlight (UVA/B intensity of 40 W/m$^2$) was sampled using 5 mL of aliquots at 1−4 min contact time points, as illustrated in Scheme 1. The solution rapidly photobleached, as illustrated in Figure 1 with 99.9% degradation after 4 min of contact time and a pseudo-first-order rate constant of 0.71 h$^{-1}$.

LC-MS characterization at the 2 min time point indicates the presence of $m/z$ values of 118.0 ($C_4H_6O_4$), 141.0 and 157.0 (Sulfone ions), 173.0 (4-amino-benzenesulfonic acid), and 189.0 (2-amino-5-hydroxy-benzenesulfonic acid) (Figure 2).[20,35,37] Neither MB nor any of the byproducts were detected after 4 min of contact time to the 0.01 ppm level of detection. These results are in accordance with previous studies of the MB photodegradation pathway by Wang et al.[35] and Gnaser et al.[37] as well as our previous batch-level study.[20] The peaks


https://doi.org/10.1021/acsestwater.1c00484
ACS EST Water 2022, 2, 786−797

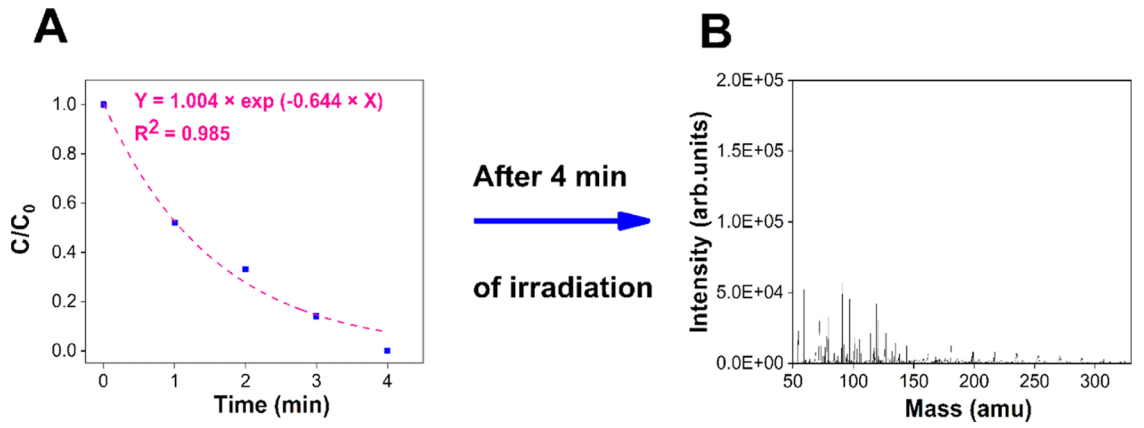


**Figure 3.** Photobleaching of 10 ppm aqueous MG in sun-flow apparatus I. (A) Photobleaching as a function of ZnO/CNF contact time and (B) LC-MS after 4 min contact time. UVA/B intensity average = 40 W/m$^2$, flow rate = 16.7 mL/min, ZnO/CNF catalyst/support used = 11.72 g, and water depth in channels ≈ 5 mm.

**Scheme 2. Photocatalytic Mechanism of ZnO for the Degradation of Organic Pollutants**[a]

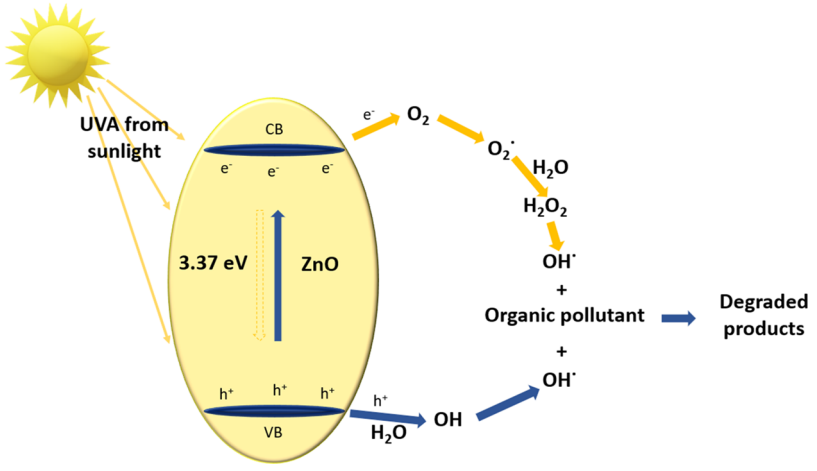


[a](Reproduced based on the mechanism proposed by Lee et al., copyright 2016[8]).

observed in the samples after 4 min of contact time (Figure 2C) are consistent with known contaminants in the Milli-Q water used (Figure 2E).

**Photocatalytic Degradation of Malachite Green (MG).** MG is in the triphenylmethane class of dyes that are highly resistant to degradation[42] and have wide application in the pulp and paper, aquaculture, and textile industries.[43] The German Federal Institute for Risk Assessment (BfR) has classified MG as an environmental contaminant that is harmful to aquaculture and the environment,[44] and toxicity has been noted toward fish.[45,46] MG byproducts can vary depending on the nature of the advanced oxidation treatment process selected, and common byproducts of the photodegradation reaction are $C_{14}H_{15}ClN_4$, $C_{19}H_{16}ClN_3$, $C_{14}H_{14}N_4$, $C_{18}H_{13}N_2$, $C_7H_8O_3$, and $C_9H_{16}O_2$.[47,48]

A 10 ppm aqueous solution of MG was flowed at a rate of 16.7 mL/min over the ZnO/CNF support. The flowing solution exposed to sunlight (UVA/B intensity of 40 W/m$^2$) was sampled using 5 mL of aliquots at 1−4 min contact time points, as illustrated in Scheme 1. The solution rapidly photobleached as illustrated in Figure 3A with >99.9% degradation after 4 min of contact time and a pseudo-first-order rate constant of 0.64 h$^{-1}$. LC-MS characterization after 4 min contact time revealed neither MG nor any of the reported byproducts to the 0.01 ppm level of detection (Figure 3B).[48,49] The detected peaks were again consistent with the trace contaminants in the Milli-Q water. Within the limits of the measurement, mineralization of MG to carbon dioxide, water, chloride, and $NO_x$ has resulted.

**Photocatalytic Degradation of Low-Concentration 1,4-Dioxane.** The concentration of 1,4-dioxane in drinking water has been reported as high as 1−5 ppm.[26] With this in mind, a ∼4 ppm concentration was used to explore the effectiveness of the ZnO/CNF catalyst in the sun-low apparatus for 1,4-dioxane removal. All samples were tested using USA-EPA Method 522 (limit of detection = 5 × 10$^{-5}$ ppm), which employs isotope dilution HRGC-MS. To measure the effect of 1,4-dioxane adsorption on the surface of the ZnO/CNF catalyst and support, the experiment was initially conducted in the dark. After 3 h of flowing, the 4 ppm aqueous solution over the catalyst bed in sun-flow apparatus I about 0.04 ppm of 1,4-dioxane (∼l% of the total sample) adsorbed on the surface of the ZnO/CNF catalyst. This observation is in contrast with our previous study,[19] where the results showed about 30% adsorption of MB on the catalyst. Therefore, it can be hypothesized based on these results that the much higher adsorption of the MB might contribute to its much more rapid degradation.


https://doi.org/10.1021/acsestwater.1c00484
ACS EST Water 2022, 2, 786−797

A 4 ppm aqueous solution of 1,4-dioxane with 2 L of total volume was flowed at a rate of 33.3 mL/min over the ZnO/CNF support for a period of 3 h (Scheme 1A). The flowing solution was exposed to sunlight, which varied over the course of the experiment with a UVA/B intensity range of 20−35 W/m$^2$. Over the first half an hour of the experiment, which corresponds to 0.7 kJ sunlight energy flux on the ZnO/CNF catalyst/support surface, about half of the 1,4-dioxane degraded. Another 2.5 h of sunlight exposure, resulting in a total energy flux over 3 h of 4.2 kJ, was required for the 1,4-dioxane concentration to decrease to 0.034 ppm or 34 $\mu$g/L (Figure 4). Overall, the pseudo-first-order rate constant for 1,4-dioxane was observed to be somewhat faster than that for the MB and Mg dyes with a value of 0.96 h$^{-1}$. The final 1,4-dioxane concentration obtained is below the lifetime health advisory level of 0.2 ppm and the $10^{-4}$ cancer risk level of 0.035 ppm advised by the USA-EPA[26] as well as the Australian Government Food Standards and WHO limitations of 0.05 ppm.

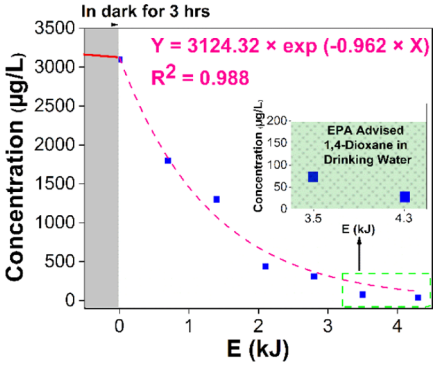


**Figure 4.** Photocatalytic degradation of 1,4-dioxane as a function of solar energy flux. UVA/B intensity varied from 20 to 35 W/m$^2$, flow rate = 33.3 mL/min or 2 L/h, catalyst used = 11.72 g, total volume of 4 ppm 1,4-dioxane sample = 2 L circulated from the treated water collection tank, and water depth in channels ≈ 5 mm.

The intermediates present in the degradation pathway were examined by LC-MS. After 1.4 kJ of total solar flux (1 h), acetic acid, oxalic acid, and ethylene glycol diformate were all detected consistent with previous literature observations (Figures S6A and S7).[50−52] Trace amounts of both oxalic acid and acetic acid remained after 4.2 kJ of total solar flux (3 h) (Figure S6B).

Based on the results from the literature, ZnO nanoflower/nanosheet catalysts showed that effective photo behaviors and O vacancy and O interstitial defects are considered as the ZnO active sites.[53−55]

**pH Study.** The pH value is a critical parameter in the photocatalytic reaction happening on the surface of the semiconductor particle. It affects the degradation process of many organic pollutants due to the amphoteric behavior of semiconductor oxides.[56−58] The pH value was controlled in all other experiments at pH 11; however, the effect of pH value on the photodegradation was investigated in the pH range of 4−14 using a constant MB concentration of 10 ppm in the flow device I under direct sunlight irradiation. The time to reach 99.99% photobleaching and the rate constant at various pH values are shown in Figure 5. In the sun-flow system using ZnO/CNF as the catalyst, the photobleaching process of the MB dye is faster in the alkaline condition (pH 8−14). The fastest degradation and lowest rate constant were at a pH of 10. This was 4 times faster than at the pH of 4.

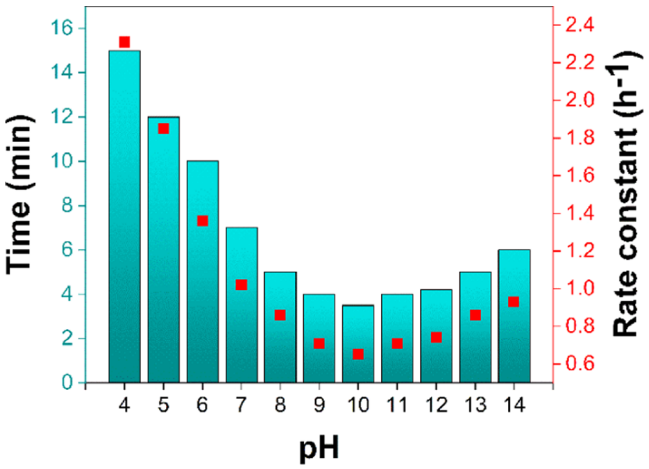


**Figure 5.** Effect of pH on the rate of MB photodegradation in the presence of ZnO/CNF catalyst. UVA/B intensity average = 80 W/m$^2$, flow rate = 16.7 mL/min, ZnO/CNF catalyst/support used = 11.72 g, and water depth in channels ≈ 5 mm.

The studies of the MB absorption on the surface of the semiconductors suggest the adsorption of $H_2O$ at the catalyst surface followed by the detachment of $OH^-$ groups, which leads to the appearance of the corresponding metal hydroxyl groups (M−OH) in the system.[16,59,60] Therefore, there is an equilibrium between the amphoteric behavior of the catalyst hydroxide and the alkali (eq 2) and acidic (eq 3) behavior of the MB in solution, which is shown as follows[60]

$$M - OH + OH^- \rightarrow M - O^- + H_2O \quad (2)$$

$$M - OH + H^+ \rightarrow M - OH - H^+ \rightarrow M - H_2O^+ \quad (3)$$

The attractive or repulsive electrostatic interactions between the organic pollutant molecules and the catalyst surface, which enhance or reduce the photodegradation process, vary with pH. The effect of pH on the degradation process is believed mainly to be a result of the ZnO surface charge and its relation with the anionic or cationic (ionic) form of the organic pollutant.[60,61] The low reaction rate at the acidic region (pH of 4−6) is because of the difference between photodissolution and dissolution of ZnO.[60,61] As MB is a material with cationic behavior, the decreased degradation time in low alkali pH values (8−11) can be attributed to the high catalyst surface hydroxylation because of the existence of large number of the hydroxyl groups. Therefore, by the formation of more radical $^{\bullet}OH$, the reaction rate is then increased. Subsequently, in the medium alkali pH range (8−12), as a result of the electrostatic attraction of the dye cations and the catalyst surface, the adsorption of the organic compound on the surface of the ZnO catalyst increases. At higher alkali pH (12−14), even though the electrostatic attraction is enhanced, at the same time, the presence of the hydroxyl groups decreases. Therefore, the reduction in the reaction rates in these pHs is attributed to the hydroxylation breakage of the catalyst surface.[16,59−61] Based on the literature[16,59−61] and the nature of ZnO semiconductor, leaching at neutral pH happens is much less compared to higher pH. Hence, it has been hypothesized that the leaching experiments at higher pH can give the results of the worst-case scenario in the photocatalytic process, and there is no need for the leaching experiments in other pH values.


https://doi.org/10.1021/acsestwater.1c00484
ACS EST Water 2022, 2, 786−797

**Leaching of ZnO Catalyst Via Photocorrosion.** Photocorrosion of ZnO to yield $Zn^{2+}$(aq) and $O_2$ is a well-documented challenge for the application of ZnO in wastewater treatment.[8,62] To investigate ZnO photocorrosion from the catalyst during the photodegradation of 1,4-dioxane, ICP-MS was performed on samples collected every 30 min for 3 h. The concentration of released $Zn^{2+}$ ions in the solution after each 30 min reading was 356, 356, 358, 367, and 391 ppb (less than $8 \times 10^{-7}$ wt % of total Zn in the catalyst), respectively. The USA-EPA guideline for zinc ions in water advises a maximum concentration of 5 ppm. Thus, the $Zn^{2+}$ release in water is about 2 orders of magnitude below the guidelines over the timeframe required to remove the 1,4-dioxane. Reusability of the catalyst over 10 cycles of MB degradation was investigated in batch mode in our previous study[20] and showed only a 2% decrease in photodegradation efficiency.

**Photodegradation as a Function of Sun-Flow Reactor Scale.** Photocatalytic water treatment offers great promise for the treatment of environmental waste; however, explicit consideration of process scaling remains an important consideration for new technologies as a substantial gap exists between small-scale laboratory batch studies[20] and a continuous, scalable flow system.[10,14] Most published photocatalytic flow processes are either not scalable, expensive to operate, or need sensitive optical equipment. Therefore, the need for a simple, cheap, and easily scalable photocatalytic treatment process is vital for the progress of this technology. Here, physical modeling principles[63] were employed to generate an additional three scales of the simple free-falling film sun-flow reactor employed in this study (Scheme 1B). Laminar flow was chosen to provide reliable residence times of the aqueous pollutant on the catalyst support and to avoid damage to the catalyst/support system with use.[14] To maintain a constant laminar flow in the channels of all apparatus during the experiments, flow rates were adjusted to maintain a Reynolds number of ~250. Although concern has been expressed about the use of dyes to test the photocatalytic activity of semiconductor oxides,[18] the experiments described above indicate very similar activity for both MB and MG as well as robust activity for 1,4-dioxane. This combination of information indicates that a dye-sensitized process is not active in these instances.

For each sun-flow apparatus, photodegradation studies of 1, 3, 5, 10, and 20 ppm aqueous solutions of MB were performed. The flowing solution exposed to sunlight (UVA/B intensity of 45 W/m$^2$) was sampled using 0.5 mL of aliquots at either a 1 min contact time point (sun-flow apparatus I) or 0.5 min contact time (sun-flow apparatus II–IV). As expected, pseudo-first-order rate constants decreased as the dimensional scale increased; however, the EE/O (kWh/m$^3$ per order) remains roughly constant at 2.1, 1.8, 1.7, and 1.5 for sun-flow apparatus I–IV, respectively (Table S1). The changes in EE/O may result from the change in channel solution depth, which was 5, 1.3, 0.5, and 0.2–0.5 mm, respectively. The decrease in solution channel depth would be expected to increase the photoflux onto the ZnO/CNF catalyst bed and to enhance oxygen availability.

To evaluate the process scale and time-dependent criteria (apparatus dimension, process time, UV intensity, and MB concentration), parameters were paired as illustrated in Figure 6. The linear trend indicates that a sufficient number of hydroxyl radicals per volume of flowing water continue to be formed as a function of increasing scale.

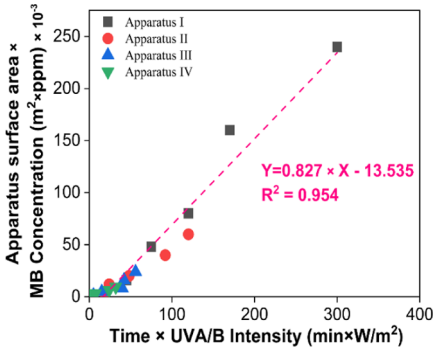


**Figure 6.** Photodegradation efficiency of MB as a function of concentration and scale for sun-flow apparatus I–IV. The rate of dye removal is dependent on dye concentration and the surface area of the ZnO/CNF catalyst system.

**Comparison to Continuous Flow Photodegradation Systems Employing ZnO and $TiO_2$ Photocatalysts.** Translation of exciting basic science advances in photocatalytic water treatment to functional systems capable of treating municipal wastewater or trade waste remains challenging.[10,14] A summary comparison of the ZnO/CNF free-falling film sun-flow apparatus described herein to continuous flow systems reported in the literature is provided in Table 2. The literature cases have been selected on the following criteria: (1) a continuous flow process; (2) earth-abundant ZnO or $TiO_2$ photocatalyst employed; and (3) MB, MG, or 1,4-dioxane degradation investigated. Based on this comparison, the ZnO-CNF sun-flow system employs a sustainable catalyst support and, to the best of our knowledge, is the first ZnO-based continuous system to achieve EPA targets for 1,4-dioxane removal. Previously, only $TiO_2$-based flow systems had achieved this goal. The ZnO-CNF sun-flow system is also notable in achieving an EE/O of 1.6 kWh/m$^3$ per order, which is only superseded by the remarkable, but more expensive and complex, $TiO_2$-P25-based system with an EE/O of 0.19 kWh/m$^3$ per order that also employed sunlight in a closed cap, Duran glass, compound parabolic collector reactor.[31] However, this study did not report the ultimate concentration to which the 1,4-dioxane was reduced. By way of comparison to continuous flow systems reported for MB and MG dye degradation, the ZnO/CNF sun-flow system is the only way to date to employ sunlight, has a superior EE/O to the UV lamp-based systems reported, and is a substantially cheaper reactor design that avoids the use of the quartz tubes common to many of the other tested systems.

**Advantages and Limitations of the Sun-Flow Apparatus.** The sun-flow apparatus described in this report employs a cheap, earth-abundant catalyst, a sustainable catalyst support material,[20] and a simple and inexpensive reactor design.[14] The open-channel, free-falling film design and the choice of ZnO photocatalyst are also optimized to take advantage of the unique UVA/B solar radiance available in the planned site location (Australia) as well as other locations with similar UVA/B radiance including most of the areas with GPS coordinates between −40 (40S) and 40 (40N) latitude.[22,23] The choice of an open-channel, sunlight-powered system has clear disadvantages in terms of reduced functionality or


https://doi.org/10.1021/acsestwater.1c00484
ACS EST Water 2022, 2, 786–797

Table 2. Comparison of Flow Reactors for Photocatalytic Degradation of MB, MG, and 1,4-Dioxane

| catalyst | earth abundant (Y/N) | support used/environmentally sustainable (Y/N) | pollutant investigated | EPA limits met (Y/N) | rate constant ($h^{-1}$) | EE/O ($kWh/m^3$/order) | source of energy | energy flux ($W/m^2$) | catalyst amount (g/l) | continuous reactor type[a] | ref |
|---|---|---|---|---|---|---|---|---|---|---|---|
| current study[b] | Y | CNF/Y | MG, MB | N/A | 0.71 | 2.2 | sunlight | 40 | 1.4 | OC/acrylic/TPFFR | |
| ZnO | Y | borosilicate glass spheres/N | MB | N/A | 1.22 | | UVA,B lamp | 50 | 6 | CC/quartz/ATFSR | 64 |
| $TiO_2$ | Y | activated carbon fiber/N | MB | N/A | 0.84 | 5.5 | UVC lamp | | 1 | CC/quartz/CIR | 65 |
| $TiO_2$/ graphene oxide/bismuth | N | Ti sheet/N | MB | N/A | 0.89 | 5.5 | UVC lamp | | | CC/acrylic/DSSR | 66 |
| ZnO@ZnS | N | silicon/N | MB | N/A | 0.13 | 13.1 | UVA lamp | 80 | 0.35 | CC/silica/AR | 67 |
| ZnO | Y | RGO/Ni/N | MG | N/A | 0.29 | 88.2 | UVA lamp | | 2 $cm^2$ | CC/glass/AFBR | 68 |
| Current study[b] | Y | CNF/Y | 1,4-dioxane | Y(0.034 ppm) | 0.96 | 1.6 | sunlight | 35 | 1.4 | OC/acrylic/TPFFR | |
| $TiO_2$ | Y | poly(vinylidene difluoride) hollow fibers/N | 1,4-dioxane | Y(0.040 ppm) | 1.8 | 1.9 | UVA | 73 | 10 g | CC/glass/MPR | 30 |
| $TiO_2$-P25 | Y | | 1,4-dioxane | | 0.11 | 0.19 | sunlight | 30 | 0.5 | CC/Duran glass/CPCR | 31 |
| $TiO_2$ | Y | | 1,4-dioxane | Y(0.09 ppm) | 0.82 | 2.88 | UVC lamp | | 13.3 | CC/Pyrex/AR | 32 |

[a]OC: open cap, CC: closed cap, TPFFR: tubular plate falling film reactor, ATFSR: annular thin-film slurry reactor, CIR: cylindrical immobilized reactor, DSSR: double skin sheet reactor, AR: annular reactor, AFBR: annular fixed bed reactor, MPR: membrane photoreactor, CPCR: compound parabolic collector reactor. [b]Data reported for sun-flow apparatus I.

complete interruption due to weather and diurnal operation. There is the potential to mitigate this disadvantage by integrating solar arrays, batteries, UVA/B lamps, and a retractable cover. Fouling from a wastewater or trade waste stream is a substantial concern for the sun-flow system presented here, although it is also a common challenge for other published reactor designs. As currently designed, the sun-flow system would best be implemented as a polishing step to remove biorecalcitrant POPs following a standard series of water treatment unit operations that remove suspended solids that scatter light and redux photoflux to the catalyst and/or remove organic biosolids that consume hydroxyl radicals need for removal of the organic pollutants of concern. This limitation is common for existing AOP photocatalytic flow-based water treatment systems.[9,10,14]

## CONCLUSIONS

The design and development of a sun-flow apparatus for high-efficacy photocatalytic degradation of low concentration 1,4-dioxane, malachite green (MG), and methylene blue (MB) in water samples were investigated. Due to the high intensity of UVA/B (360−390 nm wavelength) in the Australian regions, this UV energy from sunlight was used for the activation of the catalyst, where high efficiency with fast degradation of three investigated organic pollutants in the system was observed. The concentration of 1,4-dioxane was reduced below the limiting concentration advised by USA-EPA. The EE/O figure of merit was used to compare MB, MG, 1,4-dioxane photocatalytic degradation using ZnO/CNF catalyst sun-flow systems to previously reported continuous flow systems employing ZnO and $TiO_2$ catalysts. The sun-flow system was shown to function effectively over a scale factor of 25 in the surface area of the catalyst bed. The simple, open-channel free-falling film design effectively couples sunlight as the energy source for the photodegradation of the pollutant species.

## ASSOCIATED CONTENT

### Supporting Information

The Supporting Information is available free of charge at https://pubs.acs.org/doi/10.1021/acsestwater.1c00484.

LC-MS standard curves for MB and MG; detailed figures of the constructed sun-flow systems; results of the tests on different MB concentrations over time; qualitative LC-MS analysis results of the 1,4-dioxane samples; 1,4-dioxane degradation pathway, and EE/O and pseudo-first-order kinetic rate constants for the degradation of 10 ppm MB as a function of sun-flow apparatus scale can be found in the Supporting Information file (PDF)

## AUTHOR INFORMATION


### Corresponding Author

**Warren Batchelor** − *Bioresource Processing Research Institute of Australia, Department of Chemical and Biological Engineering, Monash University, Clayton, Victoria 3800, Australia;* orcid.org/0000-0001-6880-7765; Email: Warren.Batchelor@monash.edu

### Authors

**Mostafa Dehghani** − *Bioresource Processing Research Institute of Australia, Department of Chemical and Biological*




https://doi.org/10.1021/acsestwater.1c00484
ACS EST Water 2022, 2, 786−797

*Engineering, Monash University, Clayton, Victoria 3800, Australia;* orcid.org/0000-0001-5019-725X

**Mahdi Naseri** − *Bioresource Processing Research Institute of Australia, Department of Chemical and Biological Engineering, Monash University, Clayton, Victoria 3800, Australia;* orcid.org/0000-0001-5572-5189

**Humayun Nadeem** − *Bioresource Processing Research Institute of Australia, Department of Chemical and Biological Engineering, Monash University, Clayton, Victoria 3800, Australia*

**Mark M. Banaszak Holl** − *Bioresource Processing Research Institute of Australia, Department of Chemical and Biological Engineering, Monash University, Clayton, Victoria 3800, Australia;* orcid.org/0000-0001-7759-7456

Complete contact information is available at: https://pubs.acs.org/10.1021/acsestwater.1c00484

### Author Contributions

M.D.: investigation, experimental and analysis, writing—original draft, and review and editing. M.N.: investigation, experimental and analysis, and review and editing. H.N.: Experimental. M.M.B.H.: Supervision, writing—review and editing, and funding acquisition. W.B.: supervision, writing—review and editing, and funding acquisition.

### Notes

The authors declare no competing financial interest.

## ■ ACKNOWLEDGMENTS

The authors would like to extend their gratitude to the Australian Research Council and The ARC Research Hub for Processing Lignocellulosics into High-Value Products (PALS) for financial support through the Industry Transformation Research Hub grant for this research work (Grant: IH170100020). M. Naseri is grateful for the funding from the Australian Government Research Training Program (RTP) Scholarship. The authors are also thankful to the facilities used within the Monash University including Chemistry Department Analytical Platform and Bioprocessing Research Institute of Australia (BioPRIA).

## ■ REFERENCES

(1) Fouad, K.; Bassyouni, M.; Alalm, M. G.; Saleh, M. Y. Recent developments in recalcitrant organic pollutants degradation using immobilized photocatalysts. *Appl. Phys. A* **2021**, *127*, No. 612.

(2) Shalla, A. H.; Bhat, M. A.; Yaseen, Z. Hydrogels for removal of recalcitrant organic dyes: A conceptual overview. *J. Environ. Chem. Eng.* **2018**, *6*, 5938−5949.

(3) Shen, R.; He, K.; Zhang, A.; Li, N.; Ng, Y. H.; Zhang, P.; Hu, J.; Li, X. In-situ construction of metallic Ni3C@ Ni core−shell cocatalysts over g-C3N4 nanosheets for shell-thickness-dependent photocatalytic $H_2$ production. *Appl. Catal. B* **2021**, *291*, No. 120104.

(4) Bai, J.; Shen, R.; Chen, W.; Xie, J.; Zhang, P.; Jiang, Z.; Li, X. Enhanced photocatalytic $H_2$ evolution based on a $Ti_3C_2$/$Zn_{0.7}Cd_{0.3}S$/$Fe_2O_3$ Ohmic/S-scheme hybrid heterojunction with cascade 2D coupling interfaces. *Chem. Eng. J.* **2022**, *429*, No. 132587.

(5) Li, S.; Wang, C.; Cai, M.; Yang, F.; Liu, Y.; Chen, J.; Zhang, P.; Li, X.; Chen, X. Facile fabrication of TaON/$Bi_2MoO_6$ core−shell S-scheme heterojunction nanofibers for boosting visible-light catalytic levofloxacin degradation and Cr (VI) reduction. *Chem. Eng. J.* **2022**, *428*, No. 131158.

(6) Ren, D.; Zhang, W.; Ding, Y.; Shen, R.; Jiang, Z.; Lu, X.; Li, X. In situ fabrication of robust cocatalyst-free CdS/g-$C_3N_4$ 2D−2D step-scheme heterojunctions for highly active $H_2$ evolution. *Solar RRL* **2020**, *4*, No. 1900423.

(7) Liu, D.; Chen, S.; Li, R.; Peng, T. Review of Z-Scheme heterojunctions for photocatalytic energy conversion. *Acta Phys.-Chim. Sin.* **2021**, *37*, No. 2010017.

(8) Lee, K. M.; Lai, C. W.; Ngai, K. S.; Juan, J. C. Recent developments of zinc oxide based photocatalyst in water treatment technology: a review. *Water research* **2016**, *88*, 428−448.

(9) Oturan, M. A.; Aaron, J.-J. Advanced oxidation processes in water/wastewater treatment: principles and applications. A review. *Crit. Rev. Environ. Sci. Technol.* **2014**, *44*, 2577−2641.

(10) Loeb, S. K.; Alvarez, P. J.; Brame, J. A.; Cates, E. L.; Choi, W.; Crittenden, J.; Dionysiou, D. D.; Li, Q.; Li-Puma, G.; Quan, X. *The Technology Horizon for Photocatalytic Water Treatment: Sunrise or Sunset*; ACS Publications, 2018.

(11) He, R.; Chen, R.; Luo, J.; Zhang, S.; Xu, D. Fabrication of graphene quantum dots modified BiOI/PAN flexible fiber with enhanced photocatalytic activity. *Acta Phys.-Chim. Sin.* **2020**, *37*, No. 2011022.

(12) Liang, Z.; Shen, R.; Ng, Y. H.; Zhang, P.; Xiang, Q.; Li, X. A review on 2D $MoS_2$ cocatalysts in photocatalytic H2 production. *J. Mater. Sci. Technol.* **2020**, *56*, 89−121.

(13) Sarkar, S.; Chakraborty, S.; Bhattacharjee, C. Photocatalytic degradation of pharmaceutical wastes by alginate supported $TiO_2$ nanoparticles in packed bed photo reactor (PBPR). *Ecotoxicol. Environ. Saf.* **2015**, *121*, 263−270.

(14) Wang, D.; Mueses, M. A.; Márquez, J. A. C.; Machuca-Martínez, F.; Grčić, I.; Moreira, R. P. M.; Puma, G. L. Engineering and Modeling Perspectives on Photocatalytic Reactors for Water Treatment. *Water Res.* **2021**, *202*, No. 117421.

(15) He, X.; Wang, A.; Wu, P.; Tang, S.; Zhang, Y.; Li, L.; Ding, P. Photocatalytic degradation of microcystin-LR by modified TiO2 photocatalysis: A review. *Sci. Total Environ.* **2020**, *743*, No. 140694.

(16) Ong, C. B.; Ng, L. Y.; Mohammad, A. W. A review of ZnO nanoparticles as solar photocatalysts: Synthesis, mechanisms and applications. *Renewable Sustainable Energy Rev.* **2018**, *81*, 536−551.

(17) Fang, M.-M.; Shao, J.-X.; Huang, X.-G.; Wang, J.-Y.; Chen, W. Direct Z-scheme $CdFe_2O_4$/g-$C_3N_4$ hybrid photocatalysts for highly efficient ceftiofur sodium photodegradation. *J. Mater. Sci. Technol.* **2020**, *56*, 133−142.

(18) Barbero, N.; Vione, D. *Why Dyes Should not be Used to Test the Photocatalytic Activity of Semiconductor Oxides*; ACS Publications, 2016.

(19) Dehghani, M.; Nadeem, H.; Raghuwanshi, V. S.; Mahdavi, H.; Holl, M. M. B.; Batchelor, W. ZnO/cellulose nanofiber composites for sustainable sunlight-driven dye degradation. *ACS Appl. Nano Mater.* **2020**, *3*, 10284−10295.

(20) Dehghani, M.; Nadeem, H.; Raghuwanshi, V. S.; Mahdavi, H.; Holl, M. M. B.; Batchelor, W. ZnO/cellulose nanofiber composites for sustainable sunlight-driven dye degradation. *ACS Appl. Nano Mater.* **2020**, *3*, 10284−10295.

(21) Wang, J.; Chen, R.; Xiang, L.; Komarneni, S. Synthesis, properties and applications of ZnO nanomaterials with oxygen vacancies: A review. *Ceram. Int.* **2018**, *44*, 7357−7377.

(22) Lucas, R.; McMichael, T.; Smith, W.; Armstrong, B. K.; Prüss-Üstün, A.; Organization, W. H. *Solar Ultraviolet Radiation: Global Burden of Disease from Solar Ultraviolet Radiation*; World Health Organization, 2006.

(23) Lubin, D.; Jensen, E. H. Satellite Mapping of Solar Ultraviolet Radiation at the Earth's Surface. In *Solar Ultraviolet Radiation*; Springer, 1997; Vol. *24*, pp 95−118.

(24) Gopinathan, R.; Kanhere, J.; Banerjee, J. Effect of malachite green toxicity on non target soil organisms. *Chemosphere* **2015**, *120*, 637−644.

(25) Fischer, A.; Werner, P.; Goss, K.-U. Photodegradation of malachite green and malachite green carbinol under irradiation with different wavelength ranges. *Chemosphere* **2011**, *82*, 210−214.

(26) EPA, U. S. E. P. A. TECHNICAL FACT SHEET − 1,4-DIOXANE.

(27) Xu, X.; Liu, S.; Smith, K.; Wang, Y.; Hu, H. Light-driven breakdown of 1, 4-Dioxane for potable reuse: A review. *Chem. Eng. J.* **2019**, *373*, 508−518.
(28) Adamson, D. T.; Mahendra, S.; Walker, K. L., Jr.; Rauch, S. R.; Sengupta, S.; Newell, C. J. A multisite survey to identify the scale of the 1, 4-dioxane problem at contaminated groundwater sites. *Environ. Sci. Technol. Lett.* **2014**, *1*, 254−258.
(29) Rüdel, H.; Körner, W.; Letzel, T.; Neumann, M.; Nödler, K.; Reemtsma, T. Persistent, mobile and toxic substances in the environment: a spotlight on current research and regulatory activities. *Environ. Sci. Eur.* **2020**, *32*, No. 5.
(30) Lee, K.-C.; Beak, H.-J.; Choo, K.-H. Membrane photoreactor treatment of 1, 4-dioxane-containing textile wastewater effluent: performance, modeling, and fouling control. *Water Res.* **2015**, *86*, 58−65.
(31) Mueses, M. A.; Machuca-Martinez, F.; Puma, G. L. Effective quantum yield and reaction rate model for evaluation of photocatalytic degradation of water contaminants in heterogeneous pilot-scale solar photoreactors. *Chem. Eng. J.* **2013**, *215−216*, 937−947.
(32) Yamazaki, S.; Yamabe, N.; Nagano, S.; Fukuda, A. Adsorption and photocatalytic degradation of 1, 4-dioxane on $TiO_2$. *J. Photochem. Photobiol., A* **2007**, *185*, 150−155.
(33) Zhou, X.; Li, X.; Gao, Y.; Li, L.; Huang, L.; Ye, J. Preparation and characterization of 2D ZnO nanosheets/regenerated cellulose photocatalytic composite thin films by a two-step synthesis method. *Mater. Lett.* **2019**, *234*, 26−29.
(34) Lefatshe, K.; Muiva, C. M.; Kebaabetswe, L. P. Extraction of nanocellulose and in-situ casting of ZnO/cellulose nanocomposite with enhanced photocatalytic and antibacterial activity. *Carbohydr. Polym.* **2017**, *164*, 301−308.
(35) Wang, X.-q.; Han, S.-f.; Zhang, Q.-w.; Zhang, N.; Zhao, D.-d. In *Photocatalytic Oxidation Degradation Mechanism Study of Methylene Blue Dye Waste Water with GR/iTO2*, MATEC Web of Conferences; EDP Sciences, 2018; p 03006.
(36) Han, S.; Han, W.; Chen, J.; Sun, Y.; Dai, M.; Zhao, G. Bioremediation of malachite green by cyanobacterium Synechococcus elongatus PCC 7942 engineered with a triphenylmethane reductase gene. *Appl. Microbiol. Biotechnol.* **2020**, *104*, 3193−3204.
(37) Gnaser, H.; Savina, M. R.; Calaway, W. F.; Tripa, C. E.; Veryovkin, I. V.; Pellin, M. J. Photocatalytic degradation of methylene blue on nanocrystalline $TiO_2$: surface mass spectrometry of reaction intermediates. *Int. J. Mass Spectrom.* **2005**, *245*, 61−67.
(38) Testing, E. E. Analytical methods summaries, https://www.eurofins.com.au/environmental-testing/water-testing/. https://www.eurofins.com.au/environmental-testing/water-testing/.
(39) Xia, S.; Zhang, L.; Pan, G.; Qian, P.; Ni, Z. Photocatalytic degradation of methylene blue with a nanocomposite system: synthesis, photocatalysis and degradation pathways. *Phys. Chem. Chem. Phys.* **2015**, *17*, 5345−5351.
(40) Yu, Z.; Chuang, S. S. C. The effect of Pt on the photocatalytic degradation pathway of methylene blue over TiO2 under ambient conditions. *Appl. Catal., B* **2008**, *83*, 277−285.
(41) Rauf, M. A.; Meetani, M. A.; Khaleel, A.; Ahmed, A. Photocatalytic degradation of methylene blue using a mixed catalyst and product analysis by LC/MS. *Chem. Eng. J.* **2010**, *157*, 373−378.
(42) Song, J.; Han, G.; Wang, Y.; Jiang, X.; Zhao, D.; Li, M.; Yang, Z.; Ma, Q.; Parales, R. E.; Ruan, Z.; Mu, Y. pathway and kinetics of malachite green biodegradation by Pseudomonas veronii. *Sci. Rep.* **2020**, *10*, No. 4502.
(43) Hussain, S.; Quinn, L.; Li, J.; Casey, E.; Murphy, C. D. Simultaneous removal of malachite green and hexavalent chromium by Cunninghamella elegans biofilm in a semi-continuous system. *Int. Biodeterior. Biodegrad.* **2017**, *125*, 142−149.
(44) Malachite green identified as an environmental contaminant, https://www.bfr.bund.de/en/press_information/2007/17/malachite_green_identified_as_an_environmental_contaminant-10136.html, 2007.
(45) Sudova, E.; Machova, J.; Svobodova, Z.; Vesely, T. Negative effects of malachite green and possibilities of its replacement in the treatment of fish eggs and fish: a review. *Vet. Med.* **2008**, *52*, 527−539.
(46) Zhang, Y.; Yu, W.; Pei, L.; Lai, K.; Rasco, B. A.; Huang, Y. Rapid analysis of malachite green and leucomalachite green in fish muscles with surface-enhanced resonance Raman scattering. *Food Chem.* **2015**, *169*, 80−84.
(47) Josephine, G. A. S.; Ramachandran, S.; Sivasamy, A. Nanocrystalline ZnO doped lanthanide oxide: an efficient photocatalyst for the degradation of malachite green dye under visible light irradiation. *J. Saudi Chem. Soc.* **2015**, *19*, 549−556.
(48) Magdalane, C. M.; Kaviyarasu, K.; Vijaya, J. J.; Jayakumar, C.; Maaza, M.; Jeyaraj, B. Photocatalytic degradation effect of malachite green and catalytic hydrogenation by UV−illuminated $CeO_2$/CdO multilayered nanoplatelet arrays: investigation of antifungal and antimicrobial activities. *J. Photochem. Photobiol., B* **2017**, *169*, 110−123.
(49) Mohamed, A.; Ghobara, M. M.; Abdelmaksoud, M.; Mohamed, G. G. A novel and highly efficient photocatalytic degradation of malachite green dye via surface modified polyacrylonitrile nanofibers/biogenic silica composite nanofibers. *Sep. Purif. Technol.* **2019**, *210*, 935−942.
(50) Wang, W.; Qiao, Z.; Lee, G.-J.; Chen, H.; Ding, L.; Zhu, M.; Liu, N.; Wu, J. J. Preparation of ternary photocatalysts and their application in the degradation of 1, 4-dioxane using O3/UV/photocatalyst process. *Sep. Purif. Technol.* **2020**, *235*, No. 116194.
(51) Zeng, Q.; Dong, H.; Wang, X.; Yu, T.; Cui, W. Degradation of 1, 4-dioxane by hydroxyl radicals produced from clay minerals. *J. Hazard. Mater.* **2017**, *331*, 88−98.
(52) Beckett, M. A.; Hua, I. Elucidation of the 1, 4-dioxane decomposition pathway at discrete ultrasonic frequencies. *Environ. Sci. Technol.* **2000**, *34*, 3944−3953.
(53) Fan, J.; Li, T.; Heng, H. Hydrothermal growth of ZnO nanoflowers and their photocatalyst application. *Bull. Mater. Sci.* **2016**, *39*, 19−26.
(54) Yu, C.; Tong, Z.; Li, S.; Yin, Y. Enhancing the photocatalytic activity of ZnO by using tourmaline. *Mater. Lett.* **2019**, *240*, 161−164.
(55) Akyol, A.; Yatmaz, H. C.; Bayramoglu, M. Photocatalytic decolorization of Remazol Red RR in aqueous ZnO suspensions. *Appl. Catal., B* **2004**, *54*, 19−24.
(56) Turchi, C. S.; Ollis, D. F. Photocatalytic degradation of organic water contaminants: mechanisms involving hydroxyl radical attack. *J. Catal.* **1990**, *122*, 178−192.
(57) Sakthivel, S.; Neppolian, B.; Shankar, M. V.; Arabindoo, B.; Palanichamy, M.; Murugesan, V. Solar photocatalytic degradation of azo dye: comparison of photocatalytic efficiency of ZnO and $TiO_2$. *Sol. Energy Mater. Sol. Cells* **2003**, *77*, 65−82.
(58) Xu, B.; Ahmed, M. B.; Zhou, J. L.; Altaee, A. Visible and UV photocatalysis of aqueous perfluorooctanoic acid by $TiO_2$ and peroxymonosulfate: Process kinetics and mechanistic insights. *Chemosphere* **2020**, *243*, No. 125366.
(59) Uddin, M. M.; Hasnat, M. A.; Samed, A. J. F.; Majumdar, R. K. Influence of $TiO_2$ and ZnO photocatalysts on adsorption and degradation behaviour of Erythrosine. *Dyes Pigm.* **2007**, *75*, 207−212.
(60) Kong, J.-Z.; Li, A.-D.; Li, X.-Y.; Zhai, H.-F.; Zhang, W.-Q.; Gong, Y.-P.; Li, H.; Wu, D. Photo-degradation of methylene blue using Ta-doped ZnO nanoparticle. *J. Solid State Chem.* **2010**, *183*, 1359−1364.
(61) Poulios, I.; Avranas, A.; Rekliti, E.; Zouboulis, A. Photocatalytic oxidation of Auramine O in the presence of semiconducting oxides. *J. Chem. Technol. Biotechnol.* **2000**, *75*, 205−212.
(62) Genscher, H. Electrochemical behavior of semiconductors under illumination. *J. Electrochem. Soc.* **1966**, *113*, No. 1174.
(63) Coker, A.; Kayode, C. Scale-Up in Reactor Design. In *Modeling of Chemical Kinetics and Reactor Design*; Elsevier, 2001; pp 1034−1081.
(64) Karavasilis, M. V.; Tsakiroglou, C. D. Use of immobilized zinc oxide photocatalysts for wastewater treatment: Application to methylene blue degradation. *Can. J. Chem. Eng.* **2021**, *2016*, 1−18.


https://doi.org/10.1021/acsestwater.1c00484
*ACS EST Water* 2022, 2, 786−797

(65) Jain, P.; Kumar, A.; Verma, N.; Gupta, R. K. In-situ synthesis of TiO2 nanoparticles in ACF: Photocatalytic degradation under continuous flow. *Sol. Energy* **2019**, *189*, 35−44.
(66) Ali, I.; Kim, J.-O. Continuous-flow photocatalytic degradation of organics using modified $TiO_2$ nanocomposites. *Catalysts* **2018**, *8*, No. 43.
(67) Serrà, A.; Philippe, L. Simple and scalable fabrication of hairy ZnO@ ZnS core@ shell Cu cables for continuous sunlight-driven photocatalytic water remediation. *Chem. Eng. J.* **2020**, *401*, No. 126164.
(68) Wang, Q.; Cai, C.; Wang, M.; Guo, Q.; Wang, B.; Luo, W.; Wang, Y.; Zhang, C.; Zhou, L.; Zhang, D.; et al. Efficient photocatalytic degradation of malachite green in seawater by the hybrid of zinc-oxide nanorods grown on three-dimensional (3D) reduced graphene oxide (RGO)/Ni foam. *Materials* **2018**, *11*, No. 1004.

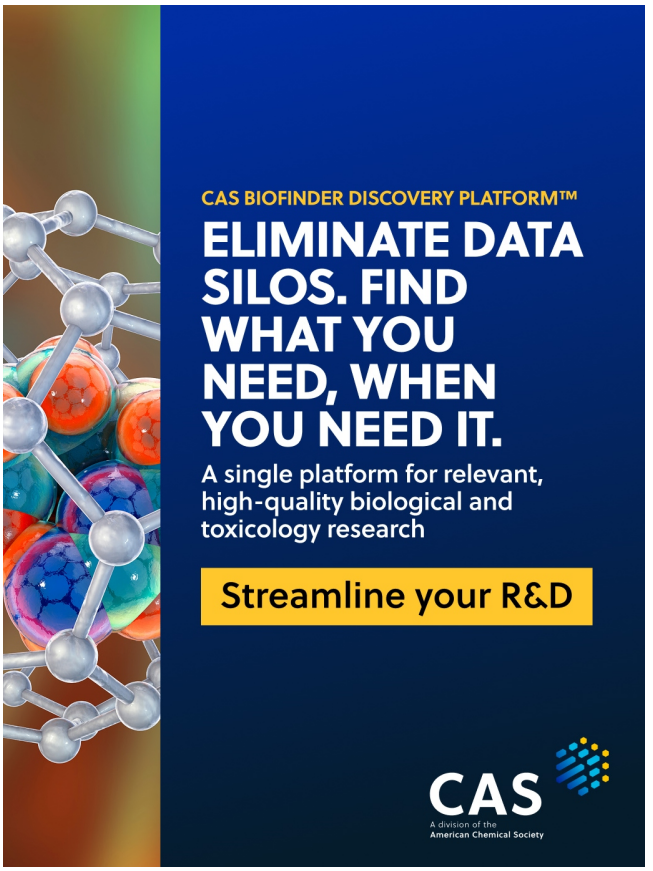




https://doi.org/10.1021/acsestwater.1c00484
*ACS EST Water* 2022, 2, 786−797